Two-photon microwave spectroscopy of Ba 6*snl* states

E. S. Shuman, J. Nunkaew, and T. F. Gallagher
Department of Physics, University of Virginia, Charlottesville, Virginia 22904-0714, USA
(Received 1 February 2007; published 17 April 2007)

We have observed Ba $6s(n+3)d\ ^1D_2-6sng\ ^1G_4$ two-photon microwave transitions for $31\leqslant n\leqslant 44$. We observe 400-kHz-wide lines in spite of the Earth's magnetic field of 0.5 G. The lines are so narrow since the transitions are between states with the same g_j factor, so that all $\Delta m_j=0$ transitions occur at the same frequency. These measurements provide an order-of-magnitude improvement in the 6*snd* quantum defects and confirm the energies predicted by a multichannel quantum defect theory analysis for this perturbed region of the spectrum.

DOI: 10.1103/PhysRevA.75.044501 PACS number(s): 32.30.Bv

I. INTRODUCTION

High-resolution spectroscopy of Rydberg states can provide a great deal of information about intra-atomic interactions. For instance, in two-electron atoms, the energies of the Rydberg states are often perturbed by interactions with states converging to other ionic limits and weak perturbations to the Rydberg states are often only observable with high-resolution spectroscopy [1,2]. The spectroscopy of Rydberg electrons can also provide information about the ions to which they are attached. From the spectroscopy of high-l states in the neutral atom the polarizability [3,4] as well as individual transition matrix elements of the ion can be extracted [5]. Precise measurements of polarizabilities and ionic multipole moments have recently become important for clocks and tests for parity violation [6,7].

Normally the the spectroscopic resolution is limited by several factors, most notably the Earth's magnetic field. In the Earth's magnetic field, transitions between Rydberg states are typically 2–3 MHz wide [4]. Usually magnetic fields must be eliminated to reduce the linewidth of these transitions; however, Li *et al.* showed that microwave resonances as narrow as 100 kHz can be observed even in magnetic field gradients as large as 10 G/cm if the initial and final states have the same l_j [8]. In their experiment they measured $ns_{1/2}\rightarrow(n+1)s_{1/2}$ and $nd_j\rightarrow(n+1)d_j$ transitions in Rb. They attributed the narrow linewidths to the fact that the initial and final states have the same g_j factor. This results in all $\Delta m_j=0$ transitions occurring at zero magnetic field frequency. They only observed narrow linewidths for transitions between states of the same l and j, but it should be possible to observe sub-MHz linewidths for microwave transitions between any states having the same g_j factor. Here we report the observation of sub-MHz linewidths in transitions between different l states with the same g_j factor. Specifically, we have observed the Ba $6s(n+3)d\ ^1D_2\rightarrow 6sng\ ^1G_4$ two-photon transitions for $n=31-44$. We observe linewidths of ~400 kHz, which is reasonably close to the transform limit (208 kHz) of the 2.4-μs microwave pulse we use. Because all singlet states have the same g_j factor, the linewidths of these transitions are not broadened by the Earth's magnetic field. The measurements presented here improve the accuracy of the $6snd\ ^1D_2$ energies by an order of magnitude [9], and they confirm the validity of a previous multichannel quantum defect theory (MQDT) analysis of these states [10]. These measurements also underscore the observation made by Li *et al.* that transitions between states having the same g_j factors are not broadened by the magnetic field. In the sections that follow we describe our experiment and present and discuss our results.

II. EXPERIMENTAL APPROACH

In the experiment a thermal beam of Ba atoms passes into the center of a box defined by brass plates as shown in Fig. 1. The box is 10 cm long by 5 cm wide by 5 cm high. The front and back plates have ~1-cm-diameter holes to allow the atomic beam and the lasers into the interaction region. The atoms are excited by two temporally overlapped 5-ns vertically polarized dye laser pulses which are counterpropagating to the atomic beam. The excitation proceeds from the ground $6s^2\ ^1S_0$ state to the $6snd\ ^1D_2$ states via the route shown in Fig. 2(a). The atoms are exposed to a 2.4-μs 10–40-GHz microwave pulse 100 ns after the laser excitation, which drives the two-photon $(n+3)d\ ^1D_2$ to $ng\ ^1G_4$ transition as indicated in Fig. 2(b). The microwaves enter the

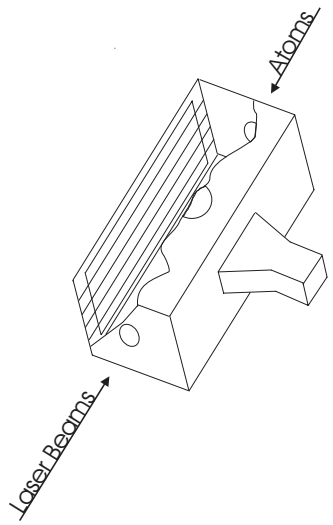

FIG. 1. Schematic diagram of the apparatus. Not shown in this figure is the multichannel plate detector which is located above the hole in the upper plate.

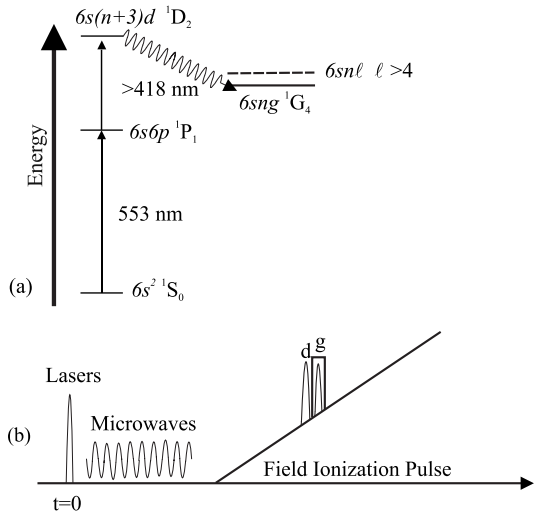

FIG. 2. (a) Energy-level diagram showing the excitation to the $6s(n+3)d\ ^1D_2$ state and subsequent microwave transition to the $6sng\ ^1G_4$ state. Due to the $6snd$ quantum defect of ~ 2.7 the $(n+3)d$ state is the nearest d state to the ng state. The dashed line indicates the energy of the hydrogenic nl states with $l>4$. (b) Timing diagram. The dye laser pulses are followed by a 2.4-μs-long microwave pulse and then a field-ionization ramp. The ng states ionize at higher fields than the $(n+3)d$ states, and the signals from the two states are easily time resolved. We gate (indicated by the black box) and record the ng signal as the microwave frequency is swept across the resonance over many shots of the laser.

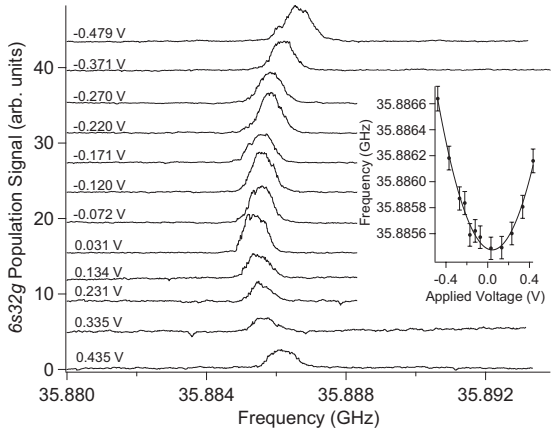

FIG. 3. Recorded $6s32g\ ^1G_4$ signal as the microwave frequency is swept through the atomic resonance at several applied bias voltages on the left plate. In the inset the positions of the resonances have been fit to a quadratic bias voltage dependence. Setting the voltage to the minimum frequency shift minimizes the stray electric field in this direction.

interaction region through a hole the size of the microwave horn in the right brass plate. The orientation of the horn creates microwaves which are vertically polarized as well. In this arrangement only $m_j=0$ states should be created; however, there is a stray magnetic field present due to a combination of the Earth's magnetic field and magnetic fields generated by labaratory equipment. We have measured the stray magnetic field to be ~ 0.5 G at an angle of $\sim 45°$ from vertical using a gaussmeter. The presence of the stray magnetic field allows the laser to create $|m_j|=0,1,2$ states and the microwaves to drive $\Delta m_j=0,\pm 1,\pm 2$ transitions. All of these transitions should be observable, but transitions other than the $\Delta m_j=0$ transitions will be spread out over a few MHz by the magnetic field. As a result only the $\Delta m_j=0$ transitions are observable in frequency scans over the atomic resonance at the lowest microwave fields. As stated previously, all of the $\Delta m_j=0$ transitions occur at zero magnetic field frequency, so these measurements give the zero magnetic field $(n+3)d\ ^1D_2-ng\ ^1G_4$ intervals.

The left brass plate has a large hole over which a grid of horizontal wires is laid. The wires are spaced by ~ 1 cm which allows vertically polarized microwaves to continue out of the interaction region without reflection. To detect the $(n+3)d\rightarrow ng$ transitions we apply a 1-μs rise-time electric-field pulse to the bottom plate immediately after the microwaves are shut off. The 600-V/cm-field pulse ionizes the $6snl$ atoms and drives the resulting electrons through a 1-cm-diameter hole in the upper plate to a dual microchannel plate detector. The combination of the laser beam diameter of 1 mm and the hole in the upper plate defines an interaction volume which is approximately a cylinder 1 mm in diameter and 1 cm long. Because atoms in ng states are harder to ionize than those in $(n+3)d$ states, the field ionization signal allows for temporal resolution of the $(n+3)d$- and ng-state signals. The ng signal is recorded with a gated integrator as the microwave frequency is swept across the atomic resonance. We average repetitive sweeps until we obtain a reasonable signal-to-noise ratio.

The microwave source is a Hewlett-Packard (HP) 8350B sweep oscillator with an 83550A 8–20-GHz plug-in, and we measure its frequency with a HP 5343A counter. The continuous-wave 10–20-GHz output of the sweep oscillator is formed into pulses with a General Microwave DM862B switch, and the pulses are transported through coaxial cable to a horn inside the vacuum chamber. To generate the 23–40-GHz microwaves the output from the General Microwave switch is sent into a Phase1 SX 40220 active doubler followed by a HP R382A precision attenuator. The result is approximately 10 mW of power at 23–40 GHz. The power is then transported by WR28 waveguide through a feedthrough to a horn inside the vacuum system.

The close proximity of the Ba $6sng$ states to the $6snh$ states means that stray electric fields in the apparatus can lead to large Stark shifts and lead to large uncertainties in the $(n+3)d-ng$ intervals we measure. For instance, a field of $E=0.05$ V/cm leads to a second-order Stark shift of $\Delta E=\frac{E^2n^7}{\Delta\delta^2}\simeq 60$ MHz for the $6s40g$ state. Here $\Delta\delta=0.04$ is the difference in quantum defect of the $6sng$ and $6snh$ states. In order to limit the effects of the stray electric fields we apply voltages to the top, left, and bottom plates to null the electric field. The other three plates remain grounded. By applying the correct voltages the stray field can theoretically be made zero in all three directions. To find the correct bias voltages to apply to the three plates we record the $(n+3)d-ng$ resonances as a function of the bias voltage in one direction, fit the frequency shift to a quadratic bias voltage dependence, and set the bias voltage at the minimum frequency shift as

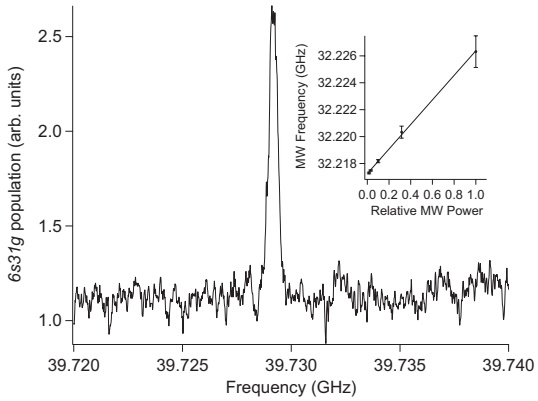

FIG. 4. Typical resonance observed after the stray field is minimized and the microwave power is reduced to produce the minimum resonance width. In this case the transition is $6s34d\ ^1D_2 \rightarrow 6s31g\ ^1G_4$. The inset illustrates the microwave power dependence of the transition.

illustrated in Fig. 3. The same procedure is used on the other plates so that the field can be made zero iteratively. The width of the transitions limits the degree to which we can minimize the stray fields. Typically the uncertainty in the centers of the transitions is approximately 40 kHz, so we cannot reduce the Stark shifts much below 40 kHz in each direction. We can estimate the residual stray electric field by adding the Stark shifts in each direction in quadrature, then determining the electric field responsible for a shift of this magnitude. For $n=32$ this results in a residual stray field of approximately $E_{stray}=\left(\frac{n^7}{\Delta\delta^2\Delta E}\right)^{-1/2}\simeq 5$ mV/cm.

III. RESULTS AND DISCUSSION

Figure 4 shows a typical resonance signal after the stray electric field has been made zero. In this case the microwave power has been reduced to the point that power broadening is eliminated. The resulting width is ~400 kHz. Additional decreases in the power do not reduce the width to the transform limit. Stark broadening from the variation in the residual stray field over the interaction volume more than likely causes the excess width. Although the power required to drive these transitions is small, ac Stark shifts are observable. To account for this shift we record the microwave transitions at several microwave powers and extrapolate to zero microwave power as shown in the inset in Fig. 4 [11].

In Table I we present the results of our measurements. Typically the centers of the transitions can be determined to less than 50 kHz; however, the uncertainty due to the stray field leads to the uncertainties given in the table. The observed intervals are given by the expression

$$\nu = R\left[\frac{1}{(n+3-\delta_d)^2}-\frac{1}{(n-\delta_g)^2}\right]. \quad (1)$$

Here δ_d and δ_g are the quantum defects of the $6s(n+3)d\ ^1D_2$ and $6sng\ ^1G_4$ states, respectively. For Ba we use the value $R=3.289\,844\times10^{15}$ Hz. We obtained this value by using R_∞ corrected by the reduced mass factor. Having been

TABLE I. Observed $(n+3)d\ ^1D_2-ng\ ^1G_4$ intervals.

n	$(n+3)d\ ^1D_2-ng\ ^1G_4$ measured interval (GHz)	Extracted $(n+3)d\ ^1D_2$ energy
31	79.4583 (1)	41922.957
32	71.7708 (1)	41929.762
34	59.2517 (2)	41941.641
35	54.1100 (3)	41946.841
36	49.5616 (3)	41951.620
37	45.5241 (4)	41956.020
39	38.6868 (5)	41963.837
40	35.7744 (6)	41967.316
41	33.1744 (8)	41970.548
42	30.8127 (9)	41973.553
43	28.6601 (11)	41976.352
44	26.7291 (12)	41978.964

measured with a high-resolution, single-frequency laser, the $6sng\ ^1G_4$–state energies are known with an accuracy of 0.006 cm^{-1} [12], while Aymar *et al.* measured the $6snd\ ^1D_2$ energies to 0.06 cm^{-1} using a pulsed laser with this resolution [9]. Because the uncertainty in the $6snd\ ^1D_2$ energies is much greater than in the $6sng\ ^1G_4$ energies, we can use the intervals of Table I along with the known $6sng\ ^1G_4$ energies to obtain the $6snd\ ^1D_2$ energies. In Table I we list the energies of the $6snd\ ^1D_2$ states extracted from the intervals of Table I using Eq. (1). Because the uncertainty in the measured intervals is at most 1 MHz, the uncertainty in the extracted energies is given by the uncertainty in the $6sng\ ^1G_4$ energy, or 0.006 cm^{-1}.

For convenience we have also plotted the energies as quantum defects in Fig. 5. To obtain the quantum defects we

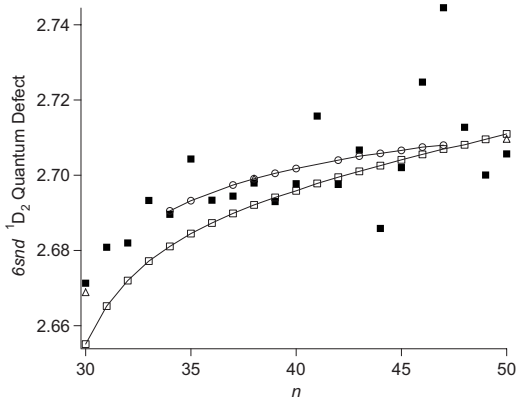

FIG. 5. Quantum defect plot of the $6snd\ ^1D_2$ states. Shown are the quantum defects extracted from the $6snd\ ^1D_2-6s(n-3)g\ ^1G_4$ intervals measured here (○), measured by Aymar *et al.* (■), calculated using MQDT by Aymar and Robaux (□), and the $n=30$, 38, and 50 quantum defects measured by Neukammer *et al.* (△). Their $n=38$ point coincides with ours. The uncertainties in the quantum defects reported here range from 0.001 at $n=34$ to 0.003 at $n=47$. Those by Neukammer *et al.* are less than 0.001 over the range of n's presented here. The uncertainties of Aymar *et al.* range from 0.005 at $n=30$ to 0.03 at $n=50$.

use the value of 42 034.902(3) cm^{-1} for the Ba^+ $6s$ limit [13]. Also shown in this plot are the previous measurements of the $6snd\ ^1D_2$ quantum defects by Aymar *et al.* [9], the results of a MQDT analysis of these data [10], and high-resolution data taken by Neukammer *et al.* of three $6snd\ ^1D_2$ states in this area [13]. Our data agree with the experimental results of Aymar *et al.* to within the relatively large uncertainty of their measurements. In a general sense our measurements confirm the results of the MQDT analysis of Aymar and Robaux. However, they also indicate that this MQDT model overstates the strength of the interactions. That is, the perturbation of the $6snd$ series by the $5d7d$ state at $n=26$ is more localized than indicated by the model. Nonetheless, the agreement of the model with the entire highly perturbed $6snd$ $J=2$ series is quite good. The high-resolution data of Neukammer *et al.* are in excellent agreement with our results. The $6s38d\ ^1D_2$ is the only state common to both sets of data, and the difference in the energy measured for this state is 0.0006 cm^{-1}. This difference is well within the ± 0.002 cm^{-1} uncertainty in their measurement and the ± 0.006 cm^{-1} uncertainty in our measurement.

IV. CONCLUSION

In conclusion, these measurements demonstrate that the technique used by Li *et al.* is not restricted to transitions between states having the same value of l and j, but may be used between any states having the same g_j factors. We have also improved the accuracy of the $6snd\ ^1D_2$ energies by several orders of magnitude, confirming the previous MQDT analysis.

ACKNOWLEDGMENT

This work has been supported by the U.S. Department of Energy.

[1] T. F. Gallagher, F. Gounand, R. Kachru, N. H. Tran, and P. Pillet, Phys. Rev. A **27**, 2485 (1983).
[2] J. A. Armstrong, J. J. Wynne, and P. Esherick, J. Opt. Soc. Am. **69**, 211 (1979).
[3] J. E. Mayer and M. G. Mayer, Phys. Rev. **43**, 605 (1933).
[4] T. F. Gallagher, R. Kachru, and N. H. Tran, Phys. Rev. A **26**, 2611 (1982).
[5] E. S. Shuman and T. F. Gallagher, Phys. Rev. A **74**, 022502 (2006).
[6] W. H. Oskay, W. M. Itano, and J. C. Bergquist, Phys. Rev. Lett. **94**, 163001 (2005).
[7] T. W. Koerber, M. Schacht, W. Nagourney, and E. N. Fortson, J. Phys. B **36**, 637 (2003).
[8] W. Li, I. Mourachko, M. W. Noel, and T. F. Gallagher, Phys. Rev. A **67**, 052502 (2003).
[9] M. Aymar, P. Camus, M. Dieulin, and C. Morillon, Phys. Rev. A **18**, 2173 (1978).
[10] M. Aymar and O. Robaux, J. Phys. B **12**, 531 (1979).
[11] S. H. Autler and C. H. Townes, Phys. Rev. **100**, 703 (1955).
[12] W. Vassen, E. Bente, and W. Hogervorst, J. Phys. B **20**, 2383 (1987).
[13] J. Neukammer, G. Jönsson, A. König, K. Vietzke, H. Hieronymus, and H. Rinneberg, Phys. Rev. A **38**, 2804 (1988).